JOURNAL OF Materials CHEMISTRY

Crystal structure of $Bi_2W_2O_9$, the $n=2$ member of the homologous series $(Bi_2O_2)B^{VI}{}_nO_{3n+1}$ of cation-deficient Aurivillius phases

Jean-Claude Champarnaud-Mesjard,[a] Bernard Frit†[a] and Akiteru Watanabe[b]

[a]*Laboratoire Science des Procédés Céramiques et de Traitements de Surface, UMR CNRS 6638, 123 avenue Albert Thomas, 87060 Limoges cedex, France. E-mail: frit@unilim.fr*
[b]*National Institute for Research in Inorganic Materials, 1–1 Namiki, Tsukuba, Ibaraki, 305–0044, Japan*

Received 5th February 1999, Accepted 7th April 1999

The crystal structure of $Bi_2W_2O_9$ has been solved by single crystal X-ray diffraction data analysis and refined to $R=0.046$ for 991 independent reflections. $Bi_2W_2O_9$ crystallizes with orthorhombic symmetry, $Pna2_1$ space group, $Z=4$, $a=5.440(1)$, $b=5.413(1)$, $c=23.740(5)$ Å. The model previously proposed by Watanabe *et al.*, *i.e.* Bi_2O_2 layers interleaved with ReO_3-like slabs of W_2O_7, has been confirmed. The distortion of the W_2O_7 octahedral network has been analysed and compared to that observed in homologous Aurivillius phases.

1 Introduction

Since the discovery of perovskite-like layered compounds by Aurivillius,[1] more than seventy phases, including a considerable number of displacive ferroelectrics (some with large spontaneous polarisation and high transition temperatures), have been found.[2]

With the general formula $Bi_2A_{n-1}B_nO_{3n+3}$ (A = Na, K, Ca, Sr, Ba, Pb, Ln, Bi, U, Th, *etc.* and B = Fe, Cr, Ga, Ti, Zr, Nb, Ta, Mo, W, *etc.*) they can be more conveniently formulated as $(Bi_2O_2)A_{n-1}B_nO_{3n+1}$, since their structures consist of perovskite-like $A_{n-1}B_nO_{3n+1}$ slabs regularly interleaved with Bi_2O_2 layers. Contrary to what was expected, the second series $Bi_2M^{VI}{}_nO_{3n+3}$ (M = Mo and W) of cation-deficient Aurivillius phases, *i.e.* consisting of the same Bi_2O_2 layers but now interleaved with ReO_3-like slabs, is far less rich since, to the best of our knowledge, only the phases corresponding to the first two terms ($n=1$ and 2; in fact the term $n=1$ is common to both series) are known. That is, only Bi_2MoO_6,[3] Bi_2WO_6 [4] and $Bi_2W_2O_9$[5,6] have been identified as cation-deficient layered structures. However, in the case of the apparently non-ferroelectric $Bi_2W_2O_9$,[5] only a model of the structure has been proposed (orthorhombic symmetry, $Pna2_1$ space group, lattice parameters: $a=5.43$, $b=5.41$, $c=23.7$ Å) on the basis of high-resolution electron microscopy images. This model had to be confirmed by a full single crystal X-ray diffraction study. This paper deals with the results of such a study.

Table 1 Crystal data and structure refinement conditions for $Bi_2W_2O_9$

Formula weight	929.66
Temperature/K	293(2)
Wavelength/Å	0.71073
Crystal system	Orthorhombic
Space group	$Pna2_1$ (33)
Unit cell dimensions: a/Å	5.440(1)
b/Å	5.413(1)
c/Å	23.740(5)
Volume/Å^3	699.1(2)
Z	4
Density (calculated)/Mg m^{-3}	8.833
Density (observed)/Mg m^{-3}	8.87(5)
Absorption coefficient/mm^{-3}	83.021
$F(000)$	1544
Crystal size/mm	$0.1\times0.05\times0.03$
θ range for data collection/°	1.72 to 29.99
Index ranges	$-1\leqslant h\leqslant7$, $-1\leqslant k\leqslant7$, $-33\leqslant l\leqslant1$
Reflections collected	1328
Independent reflections	991 [R(int) = 0.0502]
Refinement method	Full-matrix least-squares on F^2
Data/restraints/parameters	984/0/73
Goodness-of-fit on F^2 [a]	1.034
Final R indices ($I>2\sigma(I)$)[b]	$R_1=0.0458$, $wR_2=0.0925$
R indices (all data)	$R_1=0.0696$, $wR_2=0.1002$
Absolute structure parameter	0.12(8)
Extinction coefficient	0.00083(9)
Largest diff. peak and hole/e Å^{-3}	3.267 and −3.304

[a] G.O.F = $\{\sum w(F_o^2-F_c^2)/N_{obs}-N_{perm}\}^{1/2}$.
[b] $R_1(F)=\sum||F_o-F_c||/F_o||$; $wR_2(F^2)=\{\sum[w(F_o^2-F_c^2)^2]/\sum[w(F_0^2)]\}^{1/2}$.

†Corresponding author. Fax: 05 55 45 72 70.

2 Experimental

Small quantities of well formed single crystals of $Bi_2W_2O_9$ were prepared together with Bi_2WO_6 and $Bi_6Te_3W_4O_{27}$ by

Table 2 Atomic coordinates ($\times10^4$), isotropic (B_{iso}) or equivalent (B_{eq}) temperature factors (Å^2) and anisotropic displacement factors U_{ij} (Å$^2\times10^3$). The anisotropic displacement exponent takes the form $-2\pi^2[h^2a^{*2}U_{11}+.....+2hka^*b^*U_{12}]$, esds in the last digit are given in parentheses

	x	y	z	B_{eq}[a]
Bi(1)	1442(6)	4779(7)	2899(1)	1.13(7)
Bi(2)	1443(6)	9812(5)	3984(1)	1.24(7)
W(1)	1631(5)	−31(6)	1708(2)	0.50(7)
W(2)	8322(6)	5086(7)	172(2)	0.58(7)

	x	y	z	B_{iso}
O(1)	9092(60)	7600(60)	3396(15)	1.1(5)
O(2)	9371(53)	2266(50)	3401(14)	1.2(6)
O(3)	7638(71)	5544(30)	951(18)	0.9(5)
O(4)	8989(75)	1941(71)	1633(18)	1.3(7)
O(5)	671(56)	2970(55)	281(13)	1.1(6)
O(6)	7699(78)	4088(78)	9365(18)	1.8(8)
O(7)	9888(60)	7214(59)	1839(15)	0.9(4)
O(8)	9980(64)	8005(64)	96(16)	0.8(5)
O(9)	2148(52)	512(53)	2445(12)	1.1(6)

Atom	U_{11}	U_{22}	U_{33}	U_{23}	U_{13}	U_{12}
Bi(1)	16(1)	22(2)	5(1)	−3(1)	6(1)	5(1)
Bi(2)	16(1)	6(1)	25(1)	−7(1)	0(1)	−4(1)
W(1)	2(1)	10(1)	7(1)	2(1)	−1(1)	−2(1)
W(2)	13(1)	3(1)	6(1)	−2(1)	1(1)	2(1)

[a] $B_{eq}=4/3\times2\pi^2$ $(U_{11}+U_{22}+U_{33})$.

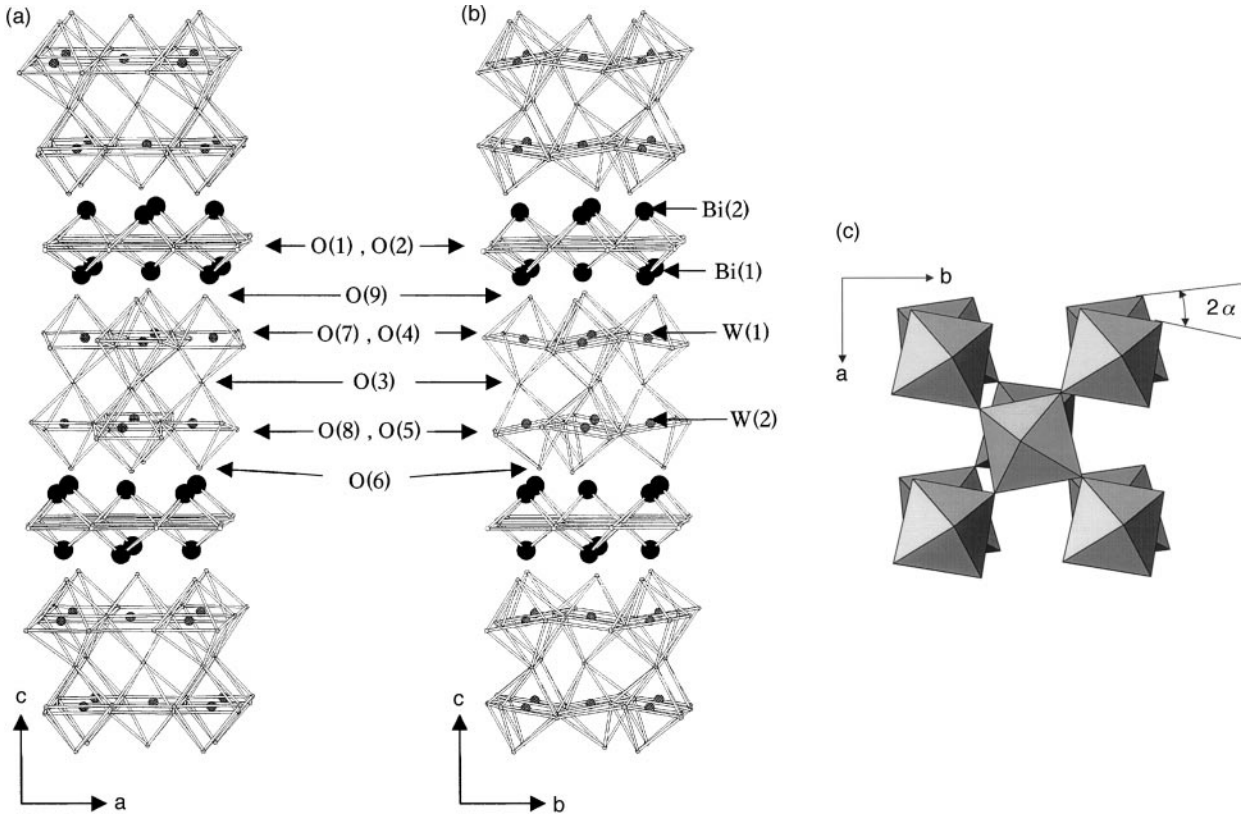

Fig. 1 Spatial views of the $Bi_2W_2O_9$ structure along (a) the *b* axis, (b) the *a* axis and (c) the *c* axis.

Table 3 Main interatomic distances (Å) and bond valences in $Bi_2W_2O_9$, esds given in parentheses

$W(1)O_6$ octahedron: $<W(1)–O> = 1.92$ Å			$W(2)O_6$ octahedron: $<W(2)–O> = 1.96$ Å		
	$d_{W–O}$	V_{ij}		$d_{W–O}$	V_{ij}
W(1)–O(3)	1.90(4)	1.06	W(2)–O(3)	1.90(4)	1,05
W(1)–O(4)	1.80(4)	1.39	W(2)–O(5)	1.73(3)	1.65
W(1)–O(4)	2.11(3)	0.59	W(2)–O(5)	2.21(3)	0.45
W(1)–O(7)	1.79(3)	1.41	W(2)–O(6)	2.01(4)	0.76
W(1)–O(7)	2.15(3)	0.53	W(2)–O(8)	1.82(3)	1.28
W(1)–O(9)	1.79(2)	1.40	W(2)–O(8)	2.10(3)	0.61
ΣV_{ij}		6.38	ΣV_{ij}		5.80
$Bi(1)O_8$ square antiprism			$Bi(2)O_8$ square antiprism		
	$d_{Bi–O}$	V_{ij}		$d_{Bi–O}$	V_{ij}
Bi(1)–O(1)	2.31(3)	0.54	Bi(2)–O(1)	2.24(3)	0.66
Bi(1)–O(1)	2.34(3)	0.50	Bi(2)–O(1)	2.39(3)	0.44
Bi(1)–O(2)	2.13(2)	0.89	Bi(2)–O(2)	2.22(3)	0.69
Bi(1)–O(2)	2.27(2)	0.60	Bi(2)–O(2)	2.63(2)	0.22
Bi(1)–O(9)	2.57(2)	0.26	Bi(2)–O(6)	2.34(4)	0.50
Bi(1)–O(9)	2.57(2)	0.26	Bi(2)–O(6)	2.46(4)	0.36
Bi(1)–O(9)	3.29(3)	0.04	Bi(2)–O(6)	3.33(3)	0.04
Bi(1)–O(9)	3.30(3)	0.04	Bi(2)–O(6)	3.45(4)	0.03
$\sum V_{ij}$		3.13	$\sum V_{ij}$		2.94

melting an intimate mixture of $3Bi_2O_3$–$4WO_3$–$5TeO_2$ at 800 °C in a gold crucible under a pure nitrogen atmosphere, and then cooling it slowly (2 °C h^{-1}) down to room temperature. The selected crystal was prismatic ($0.1 \times 0.05 \times 0.03$ mm) and apparently untwinned under polarised light. Intensity data were collected with a P4-Siemens automatic four-circle diffractometer using monochromatized Mo-Kα_1 radiation and the conditions reported in Table 1. They were corrected from adsorption effects by using a psi-scan method (XEMP program, Lamina option).[7]

3 Structure determination

The orthorhombic symmetry, the space group and the unit cell parameters previously published[5,6] were confirmed and the latter refined (Table 1). The bismuth and tungsten atoms were first located by direct methods using the SHELXTPL-PC program package.[7] A Fourier difference analysis then allowed us to locate the oxygen atoms. Successive full-matrix least-squares refinements of atomic coordinates and thermal parameters (anisotropic for Bi and W, isotropic for O atoms) for all atoms (SHELXL-93 program)[8] led to the final reliability factors $R_1 = 0.046$ and $wR_2 = 0.093$ for 991 independent reflections. The refined structural parameters are reported in Table 2. The more significant interatomic cation to anion distances and bond valences calculated by using Brown's method[9,10] are given in Table 3. Oxygen–oxygen distances are not listed but none were unusual, the shortest being 2.6 Å. CCDC reference number 1145/152. See http://www.rsc.org/suppdata/jm/1999/1319 for crystallographic files in .cif format.

4 Description of the structure

As proposed by Watanabe *et al.*,[5,6] and as shown in Fig. 1 the $Bi_2W_2O_9$ structure consists of Bi_2O_2 layers interleaved with ReO_3-like W_2O_7 sheets which are 2 octahedral layers thick. Each tungsten atom is coordinated to six oxygen atoms. The mean $<W–O>$ distances {1.92 Å for W(1) and 1.96 Å for W(2)} are in good agreement with the sum of their ionic radii as proposed by Shannon and Prewitt:[9] $r(W^{6+})_{[6]} + r(O^{2-})_{[2]} = 0.60 + 1.35 = 1.95$ Å.

By sharing O(4), O(7) [W(1)], O(8), O(5) [W(2)] corners along *x*O*y* and O(3) corners along O*z*, the octahedra constitute W_2O_7 double octahedral sheets parallel to (001). Within each octahedral layer the W(1) and W(2) atoms are set off-centre along the *a* axis toward the middle of an equatorial edge {0.47 Å for W(1) and 0.31 Å for W(2)}. The direction of this co-operative displacement is antiparallel from one octahedral

layer to the other. Such an eccentricity, more or less important, is frequently observed in simple (WO_3)[11,12] or mixed oxides (Bi_2WO_6,[4,13,14] $Bi_2Te_2WO_{10}$,[15] $Bi_2Te_3W_3O_{16}$[16]).

The Bi(1) and Bi(2) atoms are surrounded by eight oxygen atoms forming the distorted square antiprisms shown in Fig. 2. In each case two oxygen atoms do not contribute significantly to the valence bond balance (Table 3) and each bismuth atom is in fact anisotropically coordinated to only six (4+2) oxygen atoms forming a highly distorted trigonal prism. Such an anisotropy is characteristic of the important stereochemical activity of the lone pair of electrons on Bi^{3+} cations.

The bismuth atoms constitute, with the O(1) and O(2) atoms, the Bi_2O_2 layers characteristic of Aurivillius phases. These layers are weakly bound to W_2O_7 slabs *via* long Bi(1)–O(9) and Bi(2)–O(6) bonds involving the apical O(9) and O(6) atoms. Therefore, as proposed by Watanabe *et al.*,[5,6] $Bi_2W_2O_9$ can be considered as the $n=2$ member of the family $Bi_2M^{VI}{}_nO_{3n+3}$ of cation-deficient Aurivillius phases.

Examination of Fig. 1 clearly indicates that the ReO_3-like part of the structure is strongly distorted. As proposed by Withers *et al.*[17] for Bi_2WO_6, Bi_3TiNbO_9 and $Bi_4Ti_3O_{12}$ Aurivillius phases, the whole distortion can be described in terms of more or less important displacive perturbations away from a high symmetry prototype structure (space group symmetry $I4/mmm$, $a_p=b_p\approx3.85$ Å; p=perovskite) which is presumed to correspond to the crystal structure of these materials above the phase transition temperature. In the case of $Bi_2W_2O_9$, for which no voluminous A cation is present on the cuboctahedral sites of the W_2O_7 ReO_3-like slabs, we can consider that the driving forces for these distortions correspond to co-operative antiparallel displacement of W atoms along the *a* axis away from the centre of the BO_6 octahedra, and to the attraction of apical oxygen atoms of the W_2O_7 network by bismuth atoms of the Bi_2O_2 layers {see the short Bi(1)–O(6) and Bi(2)–O(9) bonds in Table 3}. We can see in Fig. 1a,b that their joint effect results, for the W(1)–O(6) and W(2)–O(6) octahedra, in: (i) an important and symmetric tilting with respect to the *b* axis (Fig. 1b), (ii) a slight and antisymmetric tilting with respect to the *a* axis (Fig. 1a) and (iii) a rotation of about $\alpha=9°$ around the *c* axis, in the opposite sense from one octahedral layer to the other and from one W_2O_7 sheet to the other, according to the space group symmetry (Fig. 1c).

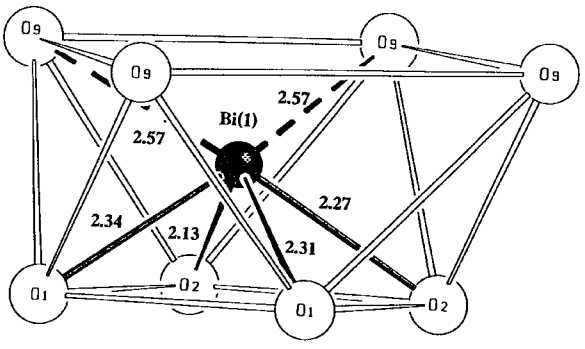

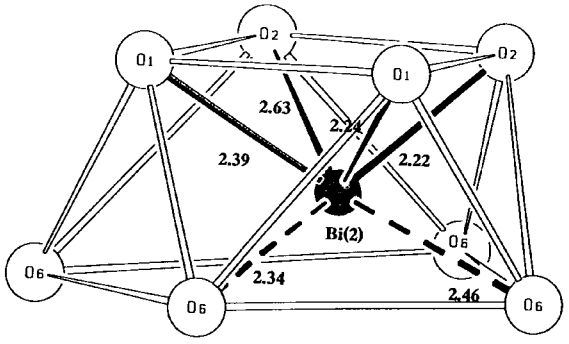

Fig. 2 The coordination polyhedra of Bi atoms. Only the shortest six Bi–O distances (Å) are indicated.

5 Comparison with the homologous $ABi_2B_2O_9$ Aurivillius phases (A = Bi,Pb,Sr,Ba; B = Nb,Ti)

In order to estimate the influence of the insertion of a cation A into the cuboctahedral cavities of the W_2O_7 octahedral framework, we have closely examined the structural parameters of $ABi_2Nb_2O_9$ Aurivillius phases whose structures have been carefully refined, *i.e.* $CaBi_2Nb_2O_9$,[18] $SrBi_2Nb_2O_9$,[18,19] $PbBi_2Nb_2O_9$,[20] Bi_3TiNbO_9[21] and $BaBi_2Nb_2O_9$.[18,19] All these phases crystallise with the $A2_1am$ space group and exhibit, as shown by Fig. 3 relative to $SrBi_2Nb_2O_9$, the same kind of distortion with respect to the prototype $I4/mmm$ structure as $Bi_2W_2O_9$ (in the case of $BaBi_2Nb_2O_9$, the most recent powder neutron diffraction study[18] suggests the ideal $I4/mmm$ space group). We must note however that because of the presence of a mirror plane perpendicular to the *c* axis all the shifts of the B atoms and all the tiltings and rotations of the octahedra are now in the same sense.

The major components of the octahedral framework distortion, *i.e.* the tilt angle around *b* and the rotation angle α around *c* are reported in Table 4 for $Bi_2W_2O_9$ and all homologous Aurivillius phases together with their unit cell parameters and volume.

From the comparison, it seems clear that the distortion decreases with the increasing size of the cation A. This is quite logical since the insertion of a voluminous cation A within the highly distorted cuboctahedra of the $Bi_2W_2O_9$ structure tends to regularise these cavities and therefore to minimise the tilts of the octahedra. This evolution is not regular because of the peculiar stereochemical behaviour of the lone pairs of the Bi^{3+} and Pb^{2+} cations. Such cations, because of their strong tendency to adopt a highly anisotropic coordination geometry, form two abnormally short bonds with the axial O(1) atoms (2×2.30 Å for Bi^{3+}, 2.35 and 2.43 Å for Pb^{2+}: distances analogous to the Sr–O(1) bonds [2.53 and 2.58 Å] of Fig. 3a,b).

These strong bonds on the one hand strengthen the tilting around the *b* axes of the octahedra and also their rotation around *c*, so justifying the high α values and therefore the abnormally low values of the *a* and *b* parameters for Bi_3NbTiO_9 and $PbBi_2Nb_2O_9$. However, on the other hand they weaken the B–O(1) bonds, so justifying the very long

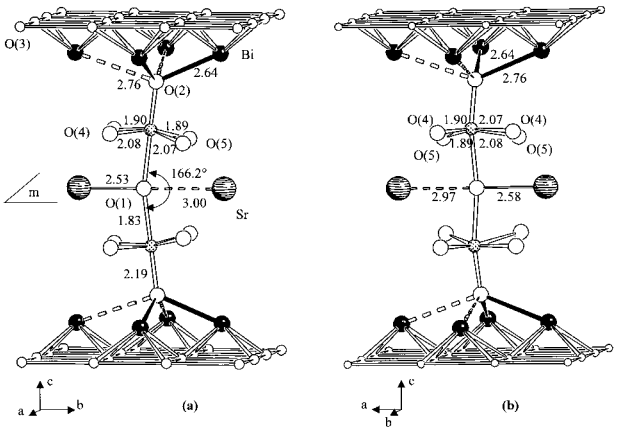

Fig. 3 Visualization of the B_2O_7 network distortion in the $SrBi_2Nb_2O_9$ structure.[19]

Table 4 Major components of the B_2O_7 octahedral framework distortion for $Bi_2W_2O_9$ and some related Aurivillius phases

Compound	Space group	Unit cell parameters/Å	V/Å^3	$r(A^{n+})_{[8]}$	B–O–B/°	α/°	Shortest A–O(1) distances/Å	
$Bi_2W_2O_9$[4,5]	$Pna2_1$	$a=5.440(1)$ $b=5.413(1)$ $c=23.740(5)$	699.08		158.7	9.5		
$CaBi_2Nb_2O_9$[18]	$A2_1am$	$a=5.4833(1)$ $b=5.4423(1)$ $c=24.8984(6)$	743.01	1.12	154.2	9.2	2.43 2.34	<2.385>
Bi_3TiNbO_9[21]	$A2_1am$	$a=5.4398(7)$ $b=5.3941(7)$ $c=25.099(5)$	736.48	1.17	160.3	8.9	2.30 2.30	<2.30>
$SrBi_2Nb_2O_9$[19]	$A2_1am$	$a=5.5189(3)$ $b=5.5154(3)$ $c=25.1124(3)$	763.42	1.26	166.2	6.2	2.53 2.58	<2.55>
$SrBi_2Nb_2O_9$[18]	$A2_1am$	$a=5.5193(3)$ $b=5.5148(3)$ $c=25.0857(6)$	763.55	1.26	165.9	6.3	2.55 2.57	<2.56>
$PbBi_2Nb_2O_9$[20]	$A2_1am$	$a=5.504(3)$ $b=5.487(3)$ $c=25.511(5)$	770.44	1.29	167.4	7.9	2.35 2.43	<2.39>
$BaBi_2Nb_2O_9$[19]	$A2_1am$	$a=5.567(1)$ $b=5.567(1)$ $c=25.634(1)$	794.44	1.42	175.7	1.9	2.59 2.73	<2.66>
$BaBi_2Nb_2O_9$[18]	$I4/mmm$	$a=5.5666(1)$ $c=25.6582(7)$	795.07	1.42	180	0		<2.78>

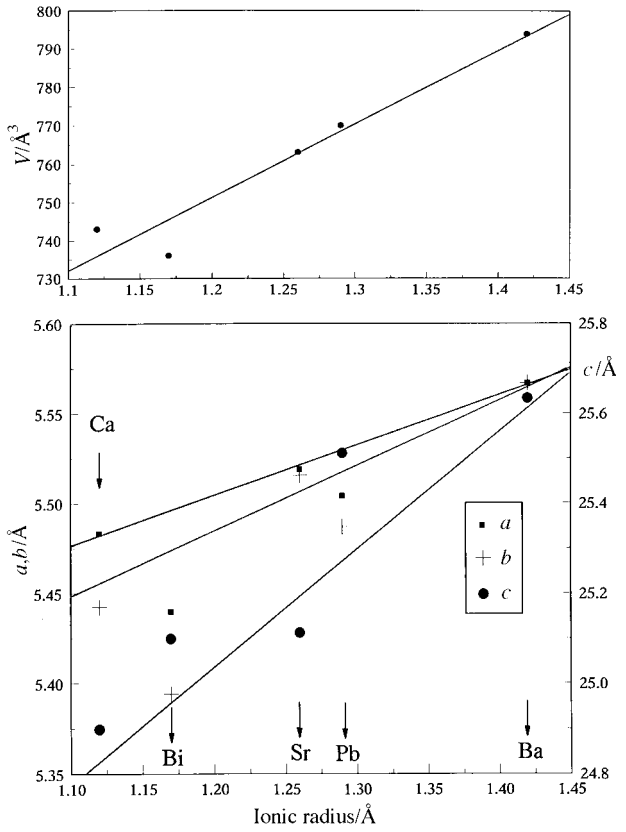

Fig. 4 Evolution of the unit cell parameters (a, b, c, V) with the ionic radius of cation A for the Aurivillius phases $CaBi_2Nb_2O_9$, $SrBi_2Nb_2O_9$, $PbBi_2Nb_2O_9$, Bi_3TiNbO_9 and $BaBi_2Nb_2O_9$.

Nb–O(1) distances (2.26 and 2.28 Å) and therefore the abnormally high values of the c parameters for Bi_3NbTiO_9 and $PbBi_2Nb_2O_9$ (Table 4 and Fig. 4).

It is somewhat surprising to note that the octahedral network distortion is nearly as important in the monoclinic ReO_3-type structure of WO_3 (rotation angle $\alpha=8.5°$, tilt angle W–O–W = 156°)[10,11] as in the $Bi_2W_2O_9$ structure despite the absence of any interaction between the Bi_2O_2 layers. This suggests that the W stereochemistry plays a major role in the distortion process. Moreover, this common distortion could explain the epitaxial growth of small WO_3 domains within the $Bi_2W_2O_9$ matrix, observed by Bando *et al.*[6] when crystals of $Bi_2W_2O_9$ suffer irradiation damage under a high-intensity electron beam.

References

1 B. Aurivillius, *Ark. Kemi*, 1949, **1**, 463; and 1951, **2**, 519.
2 B. Frit and J. P. Mercurio, *J. Alloys Compd.*, 1992, **188**, 27.
3 R. G. Teller, J. F. Brazdil, R. K. Grasseli and J. D. Jorgensen, *Acta Crystallogr., Sect. C*, 1984, **40**, 2001.
4 R. W. Wolfe, R. E. Newnham and M. I. Kay, *Solid State Commun.*, 1969, **7**, 1797.
5 A. Watanabe and M. Goto, *J. Less-Common Met.*, 1978, **61**, 265.
6 Y. Bando, A. Watanabe, Y. Sekikawa, M. Gato and S. Horiuchi, *Acta Crystallogr., Sect. A*, 1979, **35**, 142.
7 G. M. Sheldrick, SHELXTPL-PC Version 4–1, Siemens Analytical X-ray Instruments, Inc., Madison WI, 1988.
8 G. M. Sheldrick, SHELXL93, Program for refinement of crystal structures, University of Göttingen, Germany, 1993.
9 R. D. Shannon, *Acta Crystallogr., Sect. A*, 1976, **32**, 751.
10 N. E. Brese and M. O'keeffe, *Acta Crystallogr., Sect B*, 1991, **47**, 192.
11 B. O. Loopstra and P. Boldrini, *Acta Crystallogr., Sect B*, 1966, **21**, 158.
12 B. O. Loopstra and H. M. Rietveld, *Acta Crystallogr., Sect. B*, 1969, **25**, 1420.
13 K. S. Knight, *Ferroelectrics*, 1993, **150**, 319.
14 A. D. Rae, J. G. Thomson and R. L. Withers, *Acta Crystallogr., Sect. B*, 1991, **47**, 870.
15 J. C. Champarnaud-Mesjard, B. Frit, A. Chagraoui and A. Tairi, *Z. Anorg. Allg. Chem.*, 1996, **622**, 1907.
16 J. C. Champarnaud-Mesjard, B. Frit, A. Chagroui and A. Tairi, *J. Solid State Chem.*, 1996, **127**, 248.
17 R. L. Withers, J. G. Thompson and A. D. Rae, *J. Solid State Chem.*, 1991, **94**, 404.
18 S. M. Blake, M. J. Falconer, M. McCreedy and P. Lightfoot, *J. Solid State Chem.*, 1997, **7(8)**, 1609.
19 Ismunandar, B. J. Kennedy, Gunawan and Marsongkohadi, *J. Solid State Chem.*, 1996, **126**, 135.
20 V. Srikanth, H. Idink, W. B. White, E. C. Subbarao, H. Rajagopal and A. Seqeira, *Acta Crystallogr., Sect B*, 1996, **52**, 432.
21 J. G. Thompson, A. D. Rae, R. L. Withers and D. C. Craig, *Acta Crystallogr., Sect. B*, 1991, **47**, 174.

Paper 9/00992B